Carbon-Al Interface Effect on the Performance of Ionic Liquid-Based Supercapacitor at 3 V and 65 $^{\mathrm{o}}$C

Zhen-Zhen Ye

Shu-Ting Zhang

Xin-Qi Chen

Jin Wang

Ying Jin

Chao-Jie Cui
1. Department of Chemical Engineering, Tsinghua University, Beijing, 100084, China;, cuicj06@tsinghua.edu.cn

Lei Zhang

See next page for additional authors

Carbon-Al Interface Effect on the Performance of Ionic Liquid-Based Supercapacitor at 3 V and 65 $^{\mathrm{o}}$C

Authors

Zhen-Zhen Ye, Shu-Ting Zhang, Xin-Qi Chen, Jin Wang, Ying Jin, Chao-Jie Cui, Lei Zhang, Lu-Ming Qian, Gang Zhang, and Wei-Zhong Qian

Corresponding Author(s)

Chao-Jie Cui(cuicj06@tsinghua.edu.cn);
Wei-Zhong Qian(qianwz@tsinghua.edu.cn)

Carbon-Al Interface Effect on the Performance of Ionic Liquid-Based Supercapacitor at 3 V and 65 ℃

Zhen-Zhen Ye[1#], Shu-Ting Zhang[1#], Xin-Qi Chen[1], Jin Wang[1], Ying Jin[1],
Chao-Jie Cui[1*], Lei Zhang[2], Lu-Ming Qian[3], Gang Zhang[2, 3], Wei-Zhong Qian[1*]

(*1. Department of Chemical Engineering, Tsinghua University, Beijing, 100084, China;*
2. Jiangsu Zhongtian Carbonmaterial Co., Ltd., Nantong, Jiangsu, 226009, China;
3. Zhongtian Supercapacitor Technology Co., Ltd., Nantong, Jiangsu, 226009, China)

Abstract: Ionic liquid (IL) electrolyte-based supercapacitors (SCs) have advantages of high operating voltage window, high energy density and nonflammability, as compared to conventional acetonitrile-based organic electrolyte SCs, and are typically suitable for the large-scale energy storage in the era of carbon neutrality full of renewable, but unstable electricity. However, current efforts were concentrated on the study with coin-cell type of IL-SCs, and less has been reported on the pouch type of IL-SCs for a long cycling time yet. To fabricate a reliable SC for the life time test or for the accelerated aging test under high temperature, one should concern the excellent contact in the current collector/electrode interface to minimize the charge transfer resistance. In the present work, the carbon-Al interfacial effect was studied in the new SC system with Al foam as a current collector coated or painted by different carbon layers. Uniform amorphous carbon layer on Al foam was obtained from carbonization of epoxy resin film, giving a strong interaction of Al and carbon phase, as compared to that of the Al foam adhered with graphene by PVDF. In addition, to fully explore the potential of ILs electrolyte with large ion size, mesoporous carbon electrode was adopted here for a rapid ion diffusion across mesopores. Thus, the new structure SCs pouch consisting of mesoporous carbon electrode, ILs electrolyte and carbon coated-3D Al foam current collector was for the first time fabricated in the present work. Based on the as-made different pouches with capacity of 37 F, their time dependent electrochemical properties, including cyclic voltammetric (CV) response, galvanostatic charge and discharge behaviors, capacitance, contact resistance, and electrochemical impedance spectroscopic (EIS) characteristics were studied by accelerating aging test at 65 ℃ for 500 h at 3 V. The former pouch of Al foam coated with amorphous carbon layer exhibited far higher capacitance retention as compared to the pouch of Al foam adhered with graphene layer. Detailed fitting of ESR was made, and the contact resistance, charge transfer resistance, and Warburg resistance were analyzed thoroughly, providing deep insight into the strong C-Al interface effect on the high and stable performance of SCs with high energy density. Characterization of electrode sheet before and after 500 h aging test confirmed the above results. The high temperature and high voltage condition made the graphene-pasted Al foam unreliable. But the in situ coated carbon layer on Al foam exhibited relatively strong interaction and a reliable structure for the stable operation of the SCs pouch during the aging test. These solid data provide sufficient information for the further optimization of the high voltage SCs toward high energy density, high power density and long cycling time.

Key words: supercapacitor; aging test; carbon-aluminum interface; ionic liquid; aluminum foam

1 Introduction

Electrical double layer capacitors (EDLCs), also named supercapacitors (SCs), are one kind of the very important electrochemical energy storage devices with high power density and ultralong cycling life, which are widely applied for power reserve and energy storage[1-4]. Based on electrostatic interaction, EDLCs work by adsorption-desorption of electrolyte ions on the electrode surface. Electron transfer plays a key role, calling for a well interaction between the electrode material and the current collector (such as Al foil)[5-7]. For instance, the coating of carbon layer on Al foam in advance would exhibit better contact effect, thus showing much excellent electron transfer and enabling a high-rate of charge and discharge[8]. However, the typical carbon layer was always made of small particles assisted by adhesive[9], which would increase the contact resistance and introduce impurities. Recently, plasma enhanced technology allowed the direct growth of few-layer graphene on Al foil[10].

Commercial SCs always apply Al foil as the current collector, microporous activated carbon (AC) as the electrode material, and acetonitrile (ACN)-based organic liquids working at 2.7 V as the electrolyte[11-13]. With the development of SC systems, there appeared mesoporous carbon (MC) electrode material, ionic liquid (IL)-based electrolyte working at 3 ~ 4 V and three-dimension (3D) Al foam current collector[14, 15]. These functional materials would promote the SC performance in some aspects. For instance, 3D Al foam provided efficient electron transfer and heat transfer network, which avoided the overheat effect inside the electrode and alleviated the electron overpotential effect. The 3D structure also assisted in compressing the lightweight materials (such as graphene, carbon nanotubes or carbon aerogel) tightly for better performance. Moreover, the coupling of MC with ILs held a promise of high energy density SCs[16, 17].

Notably, cycling life, a key parameter of SCs, was related to the operating temperature and voltage simultaneously. Non-lineal responses of cycling life (shortened) to the coupling of temperature and voltage were observed during the accelerated aging test by using 2.7 V SCs with ACN-assisted organic electrolyte[18, 19]. Logically, long stable working time will become much serious for SCs at elevated voltage, which requires instant ion diffusion and electron transfer. To this date, rare is known for the carbon-Al foam contact effect on the performance of SCs with MC as the electrode material and IL as the electrolyte.

In this work, the comparative study on carbon-Al foam interface for the performance of SCs was reported for the first time. In detail, we created two new structures. One was to get epoxy resin on the surface of Al foam followed by high temperature (640 ℃) carbonization (denoted as Al foam@C). The other was to adhere mono-dispersed graphene on the surface of Al foam by polyvinylidene difluoride (PVDF) followed by the 110 ℃ solidification (denoted as Al foam@G). As MC was filled into the pores of 3D Al foam coated with carbon or graphene to form the electrode, the pouch-type SCs were finally made by filling IL electrolyte. Accelerated aging test results showed that the SC with Al foam@G had a worse capacitance retention after 500-hour aging. Detailed structure investigation suggested that the formation of Al-C phase in atomic scale in the sample of the Al foam@C exhibited a very stable interface under the long-time high-temperature test. These results provide insights into the interface design toward high and stable performance of SCs in the future.

2 Experimental

2.1 Preparations of Carbon-Coated Al Foams

Firstly, an epoxy resin adhesive (A component and B component, Beijng Slont Company) was dispersed with a ratio of 2:1 in alcohol and treated supersonically for 1 h. Then the Al foam was dipped into the alcohol solution for 10 s. The sample was dried at 70 ℃ for 4 h and then calcinated at 640 ℃ in Ar for 6 h. Finally, the sample of Al foam@C was obtained.

For the graphene coated Al foam, graphene prepared elsewhere[20] was ground to 2 ~ 3 μm, then dispersed in NMP solution with PVDF (PVDF:NMP = 500 mg:

10 mL) for 3 h. The Al foam was dipped into the graphene solution for 10 s and pulled out. The sample was dried at 70 °C for 4 h and then solidified at 110 °C in air for 6 h. Finally, the sample of Al foam@G was obtained.

2.2 Fabrications of Electrode based on MC and Carbon-Coated Al Foam

Main electrode material was MC prepared by the activation of commercial microporous AC with CO_2 at 950 °C for 3 ~ 4 h, as reported elsewhere[19], and the pore size distribution and Ar or N_2 adsorption-desorption curves (BET) of MC are shown in Figure S1, which was characterized by physical adsorption analyzer (Canta Instruments, QUADRASORB SI)

To make electrode, MC and super-P were dried at 250 °C under vacuum for 4 h to remove water, then cooled to ambient in Ar. Slurry was made by adding MC, super-P and PVDF with the weight ratio of 85: 7.5: 7.5 into NMP, and mechanically stirred for 4 h. The slurry had a solid concentration of 14wt.%. To obtain the electrode, the slurry was uniformly filled in the pores of the Al foam@C (or Al foam@G). Electrodes were dried at 80 °C for 12 h and then roll-pressed to be sheets of 300 ~ 400 μm. The electrode sheets were further dried at 130 °C under vacuum for 4 h.

2.3 Fabrication of SC Pouches

Electrode sheets were separated with membrane (cellulose, TF4035) and packed in the Al shell, and filled the $EMIBF_4$ electrolyte with a ratio of electrode/electrolyte of 1:5. Then the pouch was further degassed by vacuum for 24 h, and the sealed pouch remained static at 40 °C for 2 h. The capacity of the pouch was about 37 F. Here, the number of electrode sheets in each pouch was 8, while the size was 3.1 cm × 5.5 cm. Importantly, the thicknesses of the Al foam@C and Al foam@G electrode sheets were 330 μm and 400 μm, respectively. Meanwhile, the masses of loaded active material in the Al foam@C and Al foam@G electrode sheets were 1.2 g and 1.4 g, respectively.

2.4 Electrochemical Test

EIS data and CV curves at the scanning rate of 20 mV·s⁻¹ were obtained from electrochemical workstation (EC-Lab, 25 °C, Biologic, VMP-300). Galvanostatic charge and discharge curves were obtained at the current density of 1 A·g⁻¹. In addition, constant voltage charging was made for 30 min after the constant current charging, and then discharging at the constant current[19]. To evaluate the C-Al interface effect, long time cycling performance was tested at 65 °C, 3 V for 500 h. The above measured electrochemical performance data are compared and analyzed thoroughly.

3 Results

As shown in Figure 1a-b, the as-produced carbon layer carbonized *in situ* by epoxy resin on the surface
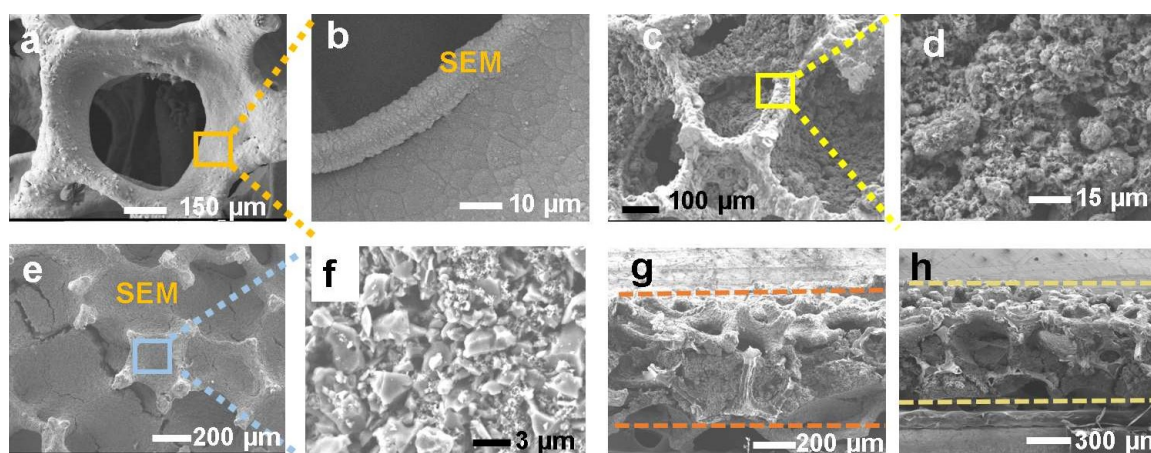
Figure 1 (a-b): SEM images of Al foam@C; (c-d): SEM images of Al foam@G; (e-f): SEM images of Al foam@C filled with MC; Cross-section SEM images of Al foam@C filled with MC (g) and Al foam@G filled with MC (h). (color on line)

of Al foam was uniform with nearly no pores observed. Besides, the carbon layer thickness could be controlled by finely modulating the amount of epoxy resin. Moreover, there was still large void to host MC particles in large amount for Al foam@C, as discussed below. For the Al foam@G, graphene in small amount was adhered onto the surface of Al foam. The interface structure of graphene and Al foam was similar to that of a graphene-Al foam sheet[14]. External surface of Al wires were entirely covered with small graphene sheet. Only when the cross-section of Al wires was cut, Al signal in dominant amount was detectable with EDS. Compared with the graphene coating layer of Al foam@G (Figure 1c-d), the carbon coating layer of Al foam@C was obviously thinner, more uniform, and much closer to the current collector. And the cross-section SEM images of Al foam@C filled with MC and Al foam@G filled with MC are exhibited in Figure 1e-g. Apparently, the filled MC slurry was more fully combined with Al foam@C, which was believed to provide excellent channels for charge transfer.

The BET specific surface area of MC used was determined to be 2745 $m^2 \cdot g^{-1}$. The pores were mainly concentrated in the range of 1 ~ 3 nm, very suitable for the diffusion of ions of EMIBF$_4$ electrolyte. In addition, its pore peak was smaller than that (4 ~ 5 nm) of a graphene nanofiber[21]. Apparently, MC in the present work gave sufficient mesopores in a small range, favorable to meet the requirements of both ion diffusion and packing density as fabricating electrode sheet. In detail, particle size of MC was in the range of 5 ~ 6 μm (Figure S2), which could be filled very tightly and uniformly inside the Al foam network (Figure 1e-f). Detailed characterization of MC around a single Al wire confirmed the densely packed structure of MC particles (Figure S2). The as-prepared electrode sheet was totally black with a surface conductance of 32000 $S \cdot cm^{-1}$, which was four orders that of MC itself. It suggested that Al wires contributed to the conductance during the test. Apparently, Al wires were not deeply embedded with MC particles, favorable to the instant electron transfer in the entire electrode area. Since the carbon layer was thin on the surface of Al foam, the electrode sheets with very close thickness and very close packing density were easily achieved. And the same weight ratio of electrolyte to electrode material was adopted, to ensure the present comparison study mainly focusing on the carbon-Al foam interface effect.

According to focused ion beam (FIB) and spherical-aberration corrected transmission electron microscope (ACTEM), the cross-section of Al-C interface of Al foam@C was also characterized successfully. Clearly, the carbon layer of Al foam@C was about 0.3 μm thick (Figure 2a). In Figure 2b, the high angle
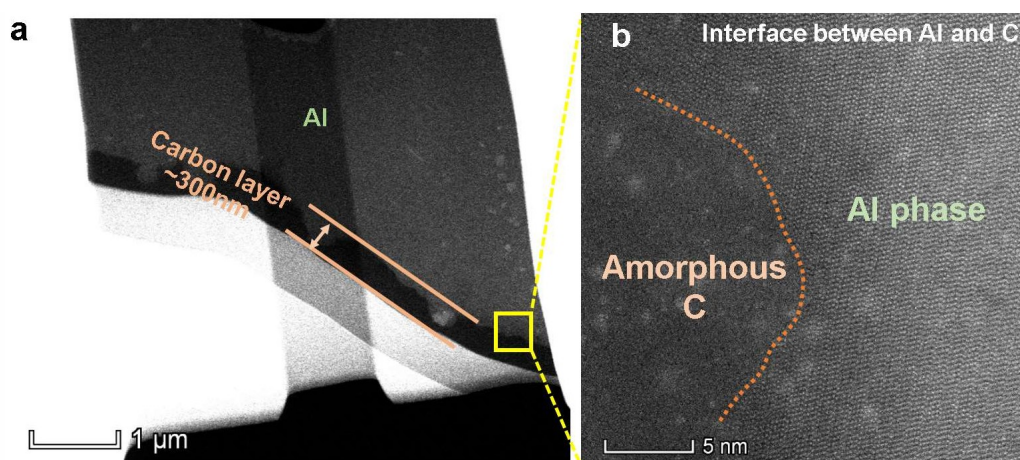
Figure 2 (a): ACTEM image of the interface of Al foam@C; (b): HAADF-ACTEM image of Al/C interface of Al foam@C. (color on line)

annular dark field (HAADF) image suggested that the strong interaction of Al-C since the Al atoms and C atoms were mixed in the interface, which was consistent with energy dispersive spectrometer (EDS) mapping image with signal interpenetration between Al element and C element (Figure S3). Apparently, the carbonization under high temperature generated the interaction, favorable to the performance of SCs as discussed later.

We compared the CV curves of different pouches to understand the electrochemical performance. The pouches were firstly treated for 2000 cycles at 25 ℃ to remove water or other impurities, and it was regarded as initial state. According to Figure 3a, CV curves showed very prefect rectangle at 20 mV·s^{-1} for pouch with Al foam@G, while the signal of pseudo-capacitance at 3 V was insignificant. After 250-hour running at 65 ℃, the pseudo-capacitance signal at 3 V became significant. The curves had a tail at 3 V and the area enclosed at 0 ~ 1 V became smaller. But the total area enclosed at 0 ~ 3 V decreased not so large. However, upon further running to 500 h, the total area enclosed at 0 ~ 3 V became much smaller, indicating the unavoidable loss of capacitance after long time cycle. Meanwhile, it was observed that the drop of voltage in the discharge curves of galvanostatic charge/discharge (GCD) became larger from < 0.2 V to > 0.5 V with the increase of aging time at 65 ℃ (Figure 3c). The associated discharge time was shortened from 80 s to less than 50 s.

In comparison, for the pouch with Al foam@C, the shape of CV curves changed insignificant after 500 h, while similar trends were observed on the GCD curves (Figure 3b and 3d). Shorter charge time was also observed with Al foam@C-based pouch, but the change was also insignificant, compared to the pouch with Al foam@G. Quantitatively, as shown in Figure 3e, the capacitance values of two pouches were 37 F and 35.8 F in the initial charge stage, respectively, which were about 1.42 times and 1.25 times that of the 2.7 V-EMIBF4 based pouch[19]. Apparently, increasing the working voltage favored the migration of ions of ILs into much relatively smaller pores of MC, enhancing the adsorption of ions of ILs on the surface
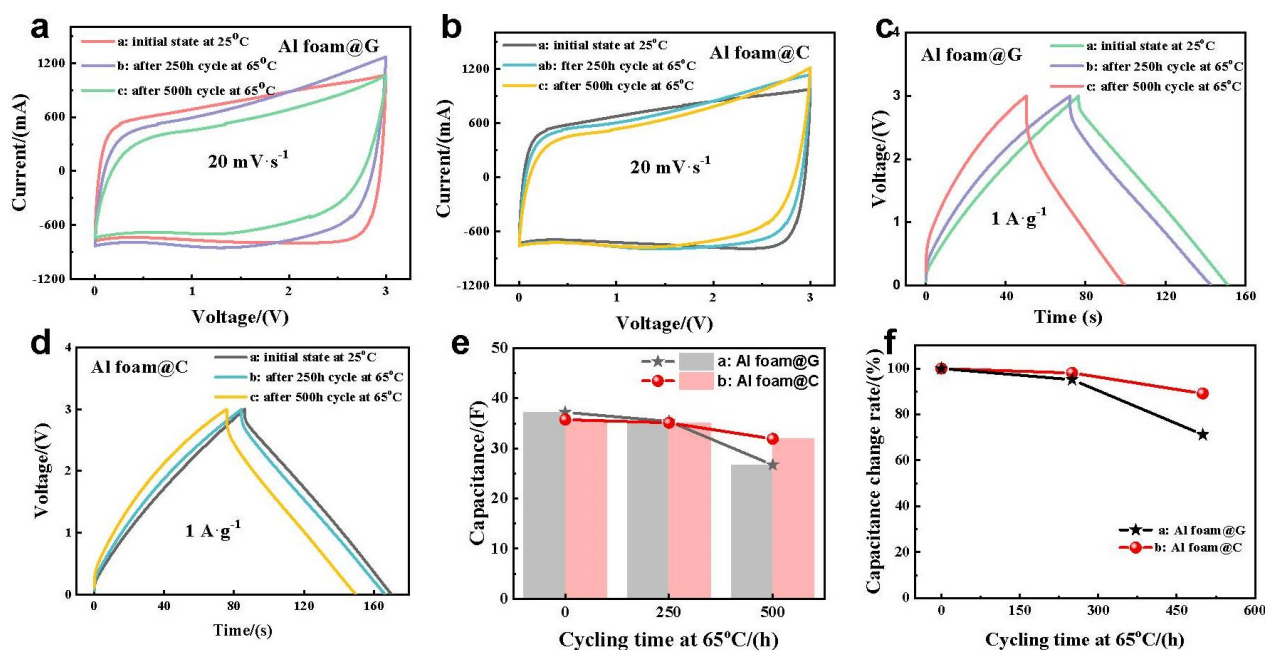
Figure 3 CV curves at 1 A g-1of Al foam@G (a) and Al foam@C (b) at initial state (25 ℃) , 250-hour cycling at 65 ℃, and 500-hour cycling at 65 ℃; GCD curves at 20 mV·s^{-1} of Al foam@G (c) and Al foam@C (d) at initial state (25 ℃) , 250-hour cycling at 65 ℃, and 500-hour cycling at 65 ℃; (e) Capacitance plots of the pouches based on Al foam@G and Al foam@G at different cycling time; (f) Capacitance change rate at different cycling time. (color on line)

of electrode and exhibiting higher capacitance response. Similar capacitance increase result was reported as elevating the cell voltage on the single walled carbon nanotube electrode[22]. It decreased slightly at 250-hour test for both, but decreased drastically at 500 h to 27 F for the pouch with Al foam@G. Capacitance retention of the pouch with Al foam@G was only 72%, much lower than that (90%) of pouch with Al foam@C (Figure 3f). Obviously, the pouch with Al foam@C exhibited much higher cycling stability at 65 ℃.

As follows, we compared the EIS results of different pouches in Figure 4. The Nyquist plots at low frequency for two pouches at initial state were much close to vertical, associated to the ideal EDLC. Performance decay, including the increases of contact resistance and the curves at low frequency, which were gradually deviated from the vertical shape occurred as increasing the cycling time. Moreover, it was obvious that the equivalent series resistance (ESR) increased with accelerated aging time at high temperature of 65 ℃. These implied the increasing serious redox reaction inside[23, 24], the decompositions of electrolyte and PVDF[25, 26], and the production of gas, which all could result in the slower ions diffusion from electrolyte to electrode[27]. In comparison, the serious deviation of pouch with Al foam@G was observed, in agreement with the resistance change from GCD tests above (Figure 3c).

To further understand the decay mechanism, Randles equivalent circuit[28-30] was used for the line-fitting of EIS curves (Figure 4d-f). In general, before the high temperature accelerated aging test, for both two pouches, ESR and charge transfer resistance (R_{ct}) were very low and close of 0.02 Ω and 0.003 Ω, respectively[31-33]. It was higher than ACN-based organic electrolyte[19] owing to the intrinsic chemistry nature of ionic liquid of EMIBF$_4$. But the ESR of the pouch at 3V was only 0.02 Ω at initial state, far smaller than that (0.03 Ω) of the pouch based on 2.7 V-EMIBF$_4$[19]. It validated the superior interface effect of Al foam with carbon layer and the enhanced adsorption effect of ions on the electrode surface as discussed above.

In addition, advantage of high stability of the pouch with Al foam@C became remarkable with the increase of cycling time. As shown in Figure 4g, its ESR was only 0.05 Ω at 500 h, much lower than that (0.09 Ω) of the pouch with Al foam@G. Similar change trend was observed for R_{ct}. There was an excellent R_{ct} of only 0.009 Ω at 500-hour cycling, much smaller than that (0.02 Ω) of Al foam@G-based pouch. Evidently, the strong interaction of carbon layer with Al in the interface shown in Figure2 was much favorable for the charge transfer. In addition, such a structure seemed to remain stable during the long-time cycling test at 65 ℃.

Perverse results were that the fitted value of Z_w (Warburg resistance) became much smaller for the pouch with Al foam@G (Figure 4h). The fitting results agreed with the rapid and short charge time as revealed in Figure 3. Z_w represents the diffusion property of ions from bulk phase to the electrode interface. Since the electrolytes in two pouches were both in the same condition of 65 ℃, their viscosities remained nearly the same and lower than those at 25 ℃. Thus, the decrease of Z_w occurred as increasing the temperature. But it was unable to explain the difference in Z_w reduction at the same operating temperature. Here, we attributed to the production of gas that was larger in the pouch with Al foam@G (Figure S4), owing to the increased contact resistance and the increased charge transfer resistance. The presence of bubbles would exhibit a stirring effect to enhance the ion movement of ILs to some degree, associated to a worsen, increased contact resistance but a lowered Warburg resistance. Gas was produced with the decomposition of electrolyte during accelerated aging test with high temperature and high voltage[25, 26]. Previous work reported that a gas as bubbles produced in the interface of current collector always resulted in the detachment of electrode layer from current collector[34, 35]. Here, the morphologies of both electrodes before and after aging were characterized. As shown in Figure S5a, a comparison of the optical photographs showed that the macroscopic morphology of the electrode with Al foam@C remained unchanged

after 500-hour aging. For the electrode with Al foam@G, the electrode material fell off more after 500-hour aging, as shown in Figure S5b. Moreover, the cross-section SEM images are shown in Figure 5. For the Al foam@C electrode, MC remained tightly attached to the Al foam skeleton after the aging test (Figure 5c-d). On the contrast, partial MC detached causing the Al skeleton to be exposed (Figure 5g-h), while the electrode material was tightly adhered on the Al foam initially (Figure 5e-f), which was the direct evidence for the failure of interface structure after aging test.

From the comprehensive analysis, bubbles exhibited a much serious negative effect, compared to their positive effect. Considering that the MC electrode

and IL electrolyte were all the same, such difference was mainly owing to the difference in carbon-Al interface of the current collector. Such comparison revealed that the strong interaction of carbon-Al interface would be crucial to the aging performance of SCs at high temperature. Here, it was also unable to exclude the possibility of decomposition of PVDF adhesive at 65 ℃ and 3 V for long time, considering frequent charge and discharge at current density of 1 $A \cdot g^{-1}$.

To this date, most of commercial organic electrolyte based SCs are unable to work at 3 V and 65 ℃ for long time, ignoring their low contact resistance. Our results suggested that the system made of MC, IL, and 3D Al foam current collector with reasonable
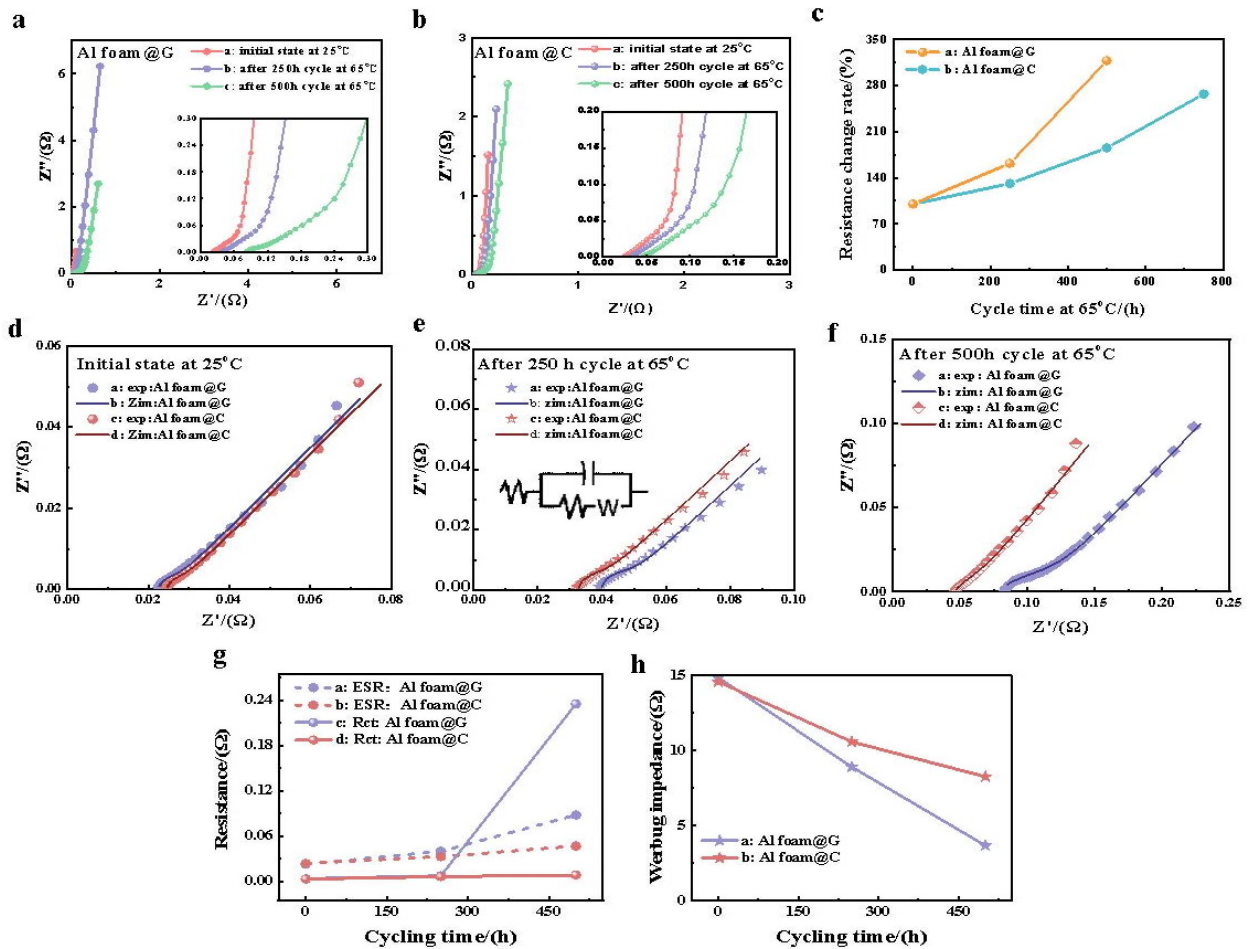
Figure 4 Nyquist plots of Al foam@G (a) and Al foam@C (b) at initial state (25 ℃), 250-hour cycling at 65 ℃, and 500-hour cycling at 65 ℃; (c) resistance change rate of two pouches at different cycling time; Nyquist plots and fitting plots of Al foam@G and Al foam@C at initial state (25 ℃) (d), 250-hour cycling at 65 ℃ (e), and 500-hour cycling at 65 ℃ (f); Comparisons of ESR and R_{ct} (g), and Z_w at different cycling time. (color on line)
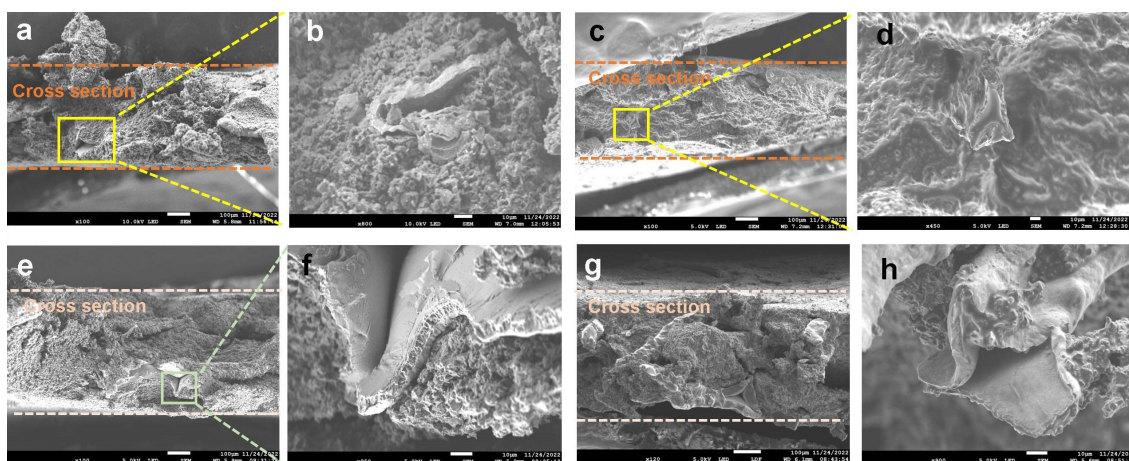
Figure 5 Comparison in SEM images of electrodes before and after aging test. (a-b): the electrode with Al foam@C before aging test; (c-d) the electrode with Al foam@C after aging test; (e-f) the electrode with Al foam@G before aging test; (g-h) the electrode with Al foam@G after aging test. (color on line)

designed structure was promising to overcome the disadvantage, which was mainly attributed to the higher chemical stability of ILs, and instant electron and heat transfer via the Al foam. Since the high voltage gave much higher energy density, our SC system deserved further study to meet more requirements in application.

4 Conclusions

The Al foam was in situ coated with carbon layer by the carbonization of epoxy resin adhesive or painted with graphene layer by PVDF adhesive. Then they were used to fill AC to fabricate the electrode sheets of a 37 F pouch with IL as the electrolyte. Aging test at 3 V and 65 ℃ was conducted and the electrochemical performances including CP, CV and EIS are compared in detail. The strong interaction of carbon-Al interface allowed the pouch exhibiting very high stability in aging test for 500 h with very small performance fluctuation. The weak interaction of graphene with Al foam by PVDF was not so strong and the PVDF tended to be decomposed in high temperature aging test. The results suggested that the carbon-Al interface structure is very crucial to the long-time cycling stability of SCs. Our SC system fabricated with MC as the electrode, ILs as the electrolyte and Al foam@C as the current collector was very promising for the high voltage application with high energy density.

References:

[1] Yang Y S. A review of electrochemical energy storage researches in the past 22 years[J]. J. Electrochem., 2020, 26 (4): 443-463.

[2] Yang Z F, Wang J, Cui C F, Jin Y, Zhang G, Zhou H H, Qian W Z. High power density & energy density Li-ion battery with aluminum foam enhanced electrode: Fabrication and simulation[J]. J. Power Sources, 2022, 524: 230977.

[3] Wang G P, Zhang L, Zhang J J. A review of electrode materials for electrochemical supercapacitors[J]. Chem. Soc. Rev., 2012, 41(2): 797-828.

[4] Zhong C, Deng Y D, Hu W B, Qiao J L, Zhang L, Zhang J J. A review of electrolyte materials and compositions for electrochemical supercapacitors[J]. Chem. Soc. Rev., 2015, 44(21): 7484-7539.

[5] Simon P, Gogotsi Y. Materials for electrochemical capacitors[J]. Nat. Mater., 2008, 7(11): 845-854.

[6] Zhu Y, Murali S, Stoller M D, Ganesh K J, Cai W, Ferreira P J, Pirkle A, Wallace R M, Cychosz K A, Thommes M, Su D, Stach E A, Ruoff R S. Carbon-based supercapacitors produced by activation of graphene[J]. Science, 2011,

332(6037): 1537-1541.

[7] Yang Z F, Tian J R, Yin Z F, Cui C J, Qian W Z, Wei F. Carbon nanotube- and graphene-based nanomaterials and applications in high-voltage supercapacitor: A review[J]. Carbon, 2019, 141: 467-480.

[8] Zhang S T, Yang Z F, Cui C J, Chen X, Yu Y T, Qian W Z, Jin Y. Ultrafast nonvolatile ionic liquids-based supercapacitors with Al foam-enhanced carbon electrode[J]. ACS Appl. Mater. Interfaces, 2021, 13(45): 53904-53914.

[9] Tian J R, Cui C J, Xie Q, Qian W Z, Xue C, Miao Y H, Jin Y, Zhang G, Guo B H. EMIMBF$_4$-GBL binary electrolyte working at −70 ℃ and 3.7 V for a high performance graphene-based capacitor[J]. J. Mater. Chem. A, 2018, 6(8): 3593-3601.

[10] Zhao Y, Liu B Z, Yi Y Y, Lian X Y, Wang M L, Li S, Yang X Z, Sun J Y. An anode-free potassium-metal battery enabled by a directly grown graphene-modulated aluminum current collector[J]. Adv. Mater., 2022, 34(29): 2202902.

[11] Fan Z J, Yan J, Wei T, Zhi L J, Ning G Q, Li T Y, Wei F. Asymmetric supercapacitors based on graphene/MnO$_2$ and activated carbon nanofiber electrodes with high power and energy density[J]. Adv. Funct. Mater., 2011, 21(12): 2366-2375.

[12] Jiang D E, Jin Z H, Henderson D, Wu J Z. Solvent effect on the pore-size dependence of an organic electrolyte supercapacitor[J]. J. Phys. Chem. Lett., 2012, 3(13): 1727-1731.

[13] Yang D F, Bock C. Laser reduced graphene for supercapacitor applications[J]. J. Power Sources, 2017, 337: 73-81.

[14] Yang Z F, Tian J R, Ye Z Z, Jin Y, Cui C J, Xie Q, Wang J, Zhang G, Dong Z Y, Miao Y H, Yu X, Qian W Z, Wei F. High energy and high power density supercapacitor with 3D Al foam-based thick graphene electrode: Fabrication and simulation[J]. Energy Stor. Mater., 2020, 33: 18-25.

[15] Li J, Wang N, Tian J R, Qian W Z, Chu W. Cross-coupled macro-mesoporous carbon network toward record high energy-power density supercapacitor at 4 V[J]. Adv. Funct. Mater., 2018, 28(51): 1806153.

[16] Li J, Zhou Y A, Tian J R, Peng L L, Deng J, Wang N, Qian W Z, Chu W. A nitrogen-doped mesopore-dominated carbon electrode allied with anti-freezing EMIBF$_4$-GBL electrolyte for superior low-temperature supercapacitors[J]. J. Mater. Chem. A, 2020, 8(20): 10386-10394.

[17] Tian J R, Cui C J, Zheng C, Qian W Z. Mesoporous tubular graphene electrode for high performance supercapacitor[J]. Chin. Chem. Lett., 2018, 29(4): 599-602.

[18] Teuber M, Strautmann M, Drillkens J, Sauer D U. Lifetime and performance assessment of commercial electric double-layer capacitors based on cover layer formation[J]. ACS Appl. Mater. & Interfaces, 2019, 11(20): 18313-18322.

[19] Ye Z Z, Chen X Q, Wang J, Li B F, Cui C J, Zhang G, Qian L M, Jin Y, Qian W Z. Evaluation of aging performance under high temperature of ionic liquid-based pouch supercapacitor[J]. CIESC Journal, 2021, 72(12): 6351-6360.

[20] Yin Z F, Shen B Y, Cui C J, Chen H, Duoni, Wang J, Qian W Z, Zhao L. High-performance graphene/carbon nanotube-based adsorbents for treating diluted O-cresol in water in a pilot-plant scale demo[J]. ACS Appl. Mater. & Interfaces, 2021, 13(36): 43266-43272.

[21] He J X, Zhao S Y, Lian Y P, Zhou M J, Wang L D, Ding B, Cui S Z. Graphene-doped carbon/Fe$_3$O$_4$ porous nanofibers with hierarchical band construction as high-performance anodes for lithium-ion batteries[J]. Electrochim. Acta, 2017, 229: 306-315.

[22] Izadi-Najafabadi A, Yamada T, Futaba D N, Hatori H, Iijima S, Hata K. Impact of cell-voltage on energy and power performance of supercapacitors with single-walled carbon nanotube electrodes[J]. Electrochem. Commun., 2010, 12(12): 1678-1681.

[23] Fernandez A P R, Périgo E A, Faria R N. Analytical expressions for electrochemical supercapacitor with potential dependent capacitance[J]. J. Energy Stor., 2021, 43: 103156.

[24] Yang Y, Fei H L, Ruan G D, Xiang C S, Tour J M. Edge-oriented MoS$_2$ nanoporous films as flexible electrodes for hydrogen evolution reactions and supercapacitor devices[J]. Adv. Mater., 2014, 26(48): 8163-8168.

[25] Ayadi M, Briat O, Lallemand R, Eddahech A, German R, Coquery G, Vinassa J M. Description of supercapacitor performance degradation rate during thermal cycling under constant voltage aging test[J]. Microelectron. Reliab., 2014, 54(9-10): 1944-1948.

[27] El Brouji H, Briat O, Vinassa J M, Bertrand N, Woirgard E. Comparison between changes of ultracapacitors model parameters during calendar life and power cycling aging tests[J]. Microelectron. Reliab., 2008, 48(8): 1473-1478.

[28] Masarapu C, Zeng H F, Hung K H, Wei B. Effect of temperature on the capacitance of carbon nanotube supercapacitors[J]. ACS Nano, 2009, 3(8): 2199-2206.

[29] Hastak R S, Sivaraman P, Potphode D D, Shashidhara K, Samui A B. All solid supercapacitor based on activated carbon and poly [2,5-benzimidazole] for high temperature application[J]. Electrochim. Acta, 2012, 59: 296-303.

[30] Poonam, Vyas M, Jangid D K, Rohan R, Pareek K. Investigation of supercapacitor cyclic degradation through impedance spectroscopy and randles circuit model [J]. Energy Stor., 2022, 4(5): e355.

[31] Saha P, Dey S, Khanra M. Second-life applications of supercapacitors: Effective capacitance prognosis and aging [J]. J. Power Sources, 2021, 496: 229824.

[32] Jossen A. Fundamentals of battery dynamics[J]. J. Power Sources, 2006, 154(2): 530-538.

[33] Yang C Z, Li C Y V, Li F J, Chan K Y. Complex impedance with transmission line model and complex capacitance analysis of ion transport and accumulation in hierarchical core-shell porous carbons[J]. J. Electrochem. Soc., 2013, 160(4): H271-H278.

[34] Li J, Xu Z, Zhang Z A. In situ combined analysis of gases and electrochemical signals of an activated carbon-based supercapacitor at 2.7-4 V[J]. RSC Adv., 2018, 8(56): 32188-32192.

[35] Kim H S, Kim Y H, Roh K C, Kim K B. Sandwich-type ordered mesoporous carbon/graphene nanocomposites derived from ionic liquid[J]. Nano Res., 2016, 9(9): 2696-2706.

基于离子液体的超级电容在 3 V 及 65 ℃ 老化条件下的铝碳界面效应

叶珍珍[1#]，张抒婷[1#]，陈鑫祺[1]，王 瑾[1]，金 鹰[1]，崔超婕[1*]，
张 磊[2]，钱陆明[3]，张 刚[2,3]，骞伟中[1*]

(1. 清华大学化工系, 北京 100084, 中国; 2. 江苏中天碳基材料有限公司, 江苏 南通 226009, 中国;
3. 中天超容科技有限公司, 江苏 南通, 226009, 中国)

摘要：相比于传统乙腈电解液体系的超级电容器，离子液体基超级电容器具有工作窗口电压高，能量密度大，不可燃等优点，适用于碳中和时代清洁但不稳定电力领域的大规模储能。然而，目前的工作主要集中在对纽扣型离子液体-超级电容器的研究上，有关软包式离子液体-超级电容器的长循环寿命评测的报道较少。构建可靠的超级电容器用于长时间测试或在高温下开展加速老化测试，应考虑集流体/电极界面的良好接触，以最小化电荷转移电阻。本文以包覆不同碳层的泡沫铝为集流体，研究了超级电容器新系统中的碳-铝界面效应。通过环氧树脂薄膜碳化得到的均匀无定形碳层，相比通过 PVDF 粘附石墨烯碳层，赋予了铝相和碳相更强的相互作用。此外，为了充分挖掘大离子尺寸的离子液体电解液的潜力，本文采用介孔碳电极实现离子在介孔间的快速扩散。因此，本工作首次制备了由介孔碳电极、离子液体电解液和覆碳三维泡沫铝集流体组成的新结构软包式超级电容器。以自制的容量为 37 F 的不同软包式超级电容器件，通过 3 V、65 ℃、500 h 加速老化试验，研究了其时间依赖性的电化学性能，包括 CV 测试、恒流充放电测试、电容值、接触电阻、电化学阻抗谱等。相比石墨烯包覆的泡沫铝基器件，无定形碳层包覆的泡沫铝基器件表现出更高的电容保持率。此外，我们还对 ESR 进行了等效电路拟合，并深入分析了接触电阻、电荷转移电阻、韦伯电阻，研究了 C-Al 界面对高能量密度超级电容器的高性能和稳定性的影响。500 小时老化测试前后的极片表征证实了上述结果。高温、高压条件使粘附石墨烯碳层的泡沫铝界面结构不可靠。而泡沫铝表面原位包覆的碳层在老化过程中表现出较强的相互作用和稳定的结构。这些坚实的数据为面向高能量密度、高功率密度和长循环寿命，进一步优化高窗口电压超级电容器提供了充足的信息。

关键词：超级电容器；老化试验；碳-铝界面；离子液体；泡沫铝